Timelike Compton Scattering

Jakub Wagner

Theoretical Physics Department
National Centre for Nuclear Research, Warsaw

Dilepton workshop, IJClab, 25th November, 2021

In collaboration with:
B. Pire, L. Szymanowski, P.Sznajder, H. Moutarde, O. Grocholski

In addition to spacelike DVCS ...

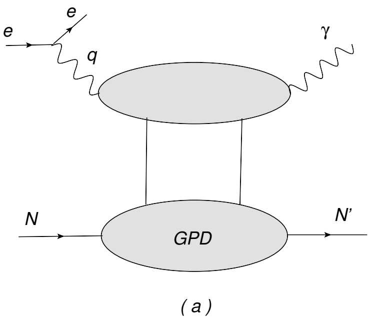

Figure: Deeply Virtual Compton Scattering (DVCS) : $lN \to l'N'\gamma$

we MUST also study timelike DVCS

Berger, Diehl, Pire, 2002

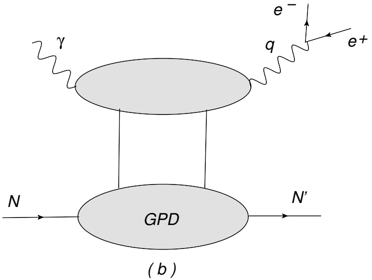

Figure: Timelike Compton Scattering (TCS): $\gamma N \to l^+ l^- N'$

Why TCS:

- same proven factorization properties as DVCS
- universality of the GPDs
- another source for GPDs (special sensitivity on real part of GPD H),
- the same final state as in J/ψ, but cleaner theoretical description!

Exciting times - DATA arrives !!!

- CLAS12 - first measurement of TCS! $\rightarrow$ P.Chatagnon talk
- Prospects for EIC $\rightarrow$ D.Sokhan talk

Coefficient functions and Compton Form Factors

CFFs are the GPD dependent quantities which enter the amplitudes. They are defined through relations:

$$\mathcal{A}^{\mu\nu}(\xi,t) = -e^2 \frac{1}{(P+P')^+}\,\bar{u}(P')\left[g_T^{\mu\nu}\left(\mathcal{H}(\xi,t)\,\gamma^+ + \mathcal{E}(\xi,t)\,\frac{i\sigma^{+\rho}\Delta_\rho}{2M}\right) + i\epsilon_T^{\mu\nu}\left(\widetilde{\mathcal{H}}(\xi,t)\,\gamma^+\gamma_5 + \widetilde{\mathcal{E}}(\xi,t)\,\frac{\Delta^+\gamma_5}{2M}\right)\right] u(P)\,,$$

where:

$$\begin{aligned}
\mathcal{H}(\xi,t) &= +\int_{-1}^{1} dx \left(\sum_q T^q(x,\xi)H^q(x,\xi,t) + T^g(x,\xi)H^g(x,\xi,t)\right)\\
\widetilde{\mathcal{H}}(\xi,t) &= -\int_{-1}^{1} dx \left(\sum_q \widetilde{T}^q(x,\xi)\widetilde{H}^q(x,\xi,t) + \widetilde{T}^g(x,\xi)\widetilde{H}^g(x,\xi,t)\right).
\end{aligned}$$

Spacelike vs Timelike

D.Mueller, B.Pire, L.Szymanowski, J.Wagner, Phys.Rev.D86, 2012.

Thanks to simple spacelike-to-timelike relations, we can express the timelike CFFs by the spacelike ones in the following way:

$$
\begin{aligned}
{}^{T}\mathcal{H} &\overset{\text{LO}}{=} {}^{S}\mathcal{H}^{*}\,, \\
{}^{T}\widetilde{\mathcal{H}} &\overset{\text{LO}}{=} -{}^{S}\widetilde{\mathcal{H}}^{*}\,, \\
{}^{T}\mathcal{H} &\overset{\text{NLO}}{=} {}^{S}\mathcal{H}^{*} - i\pi\, \mathcal{Q}^2 \frac{\partial}{\partial \mathcal{Q}^2} {}^{S}\mathcal{H}^{*}\,, \\
{}^{T}\widetilde{\mathcal{H}} &\overset{\text{NLO}}{=} -{}^{S}\widetilde{\mathcal{H}}^{*} + i\pi\, \mathcal{Q}^2 \frac{\partial}{\partial \mathcal{Q}^2} {}^{S}\widetilde{\mathcal{H}}^{*}\,.
\end{aligned}
$$

The corresponding relations exist for (anti-)symmetric CFFs $\mathcal{E}$ ($\widetilde{\mathcal{E}}$).

DVCS CFFs from Artificial Neural Network fit - PARTONS

H. Moutarde, P. Sznajder, J. Wagner, Eur.Phys.J. C79 (2019)

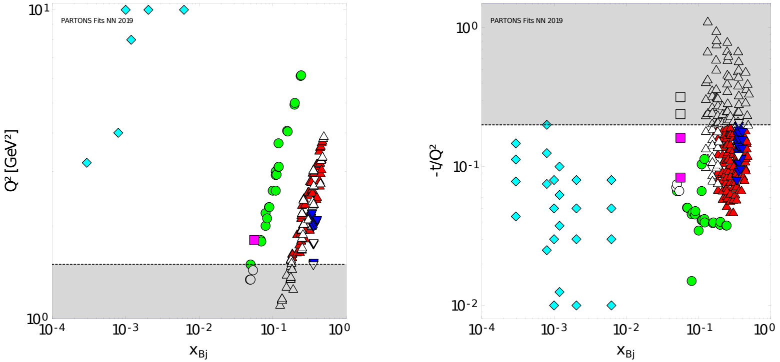

Figure: Coverage of the (x_{Bj}, Q^2) (left) and $(x_{\mathrm{Bj}}, -t/Q^2)$ (right) phase-spaces by the experimental data used in DVCS CFFs fit. The data come from the Hall A (▼, ▽), CLAS (▲, △), HERMES (●, ○), COMPASS (■, □) and HERA H1 and ZEUS (♦, ◊) experiments. The gray bands (open markers) indicate phase-space areas (experimental points) being excluded from this analysis due to the cuts.

DVCS vs TCS CFFs

O. Grocholski, H. Moutarde, B. Pire, P. Sznajder, J. Wagner, Eur.Phys.J. C80 (2020)

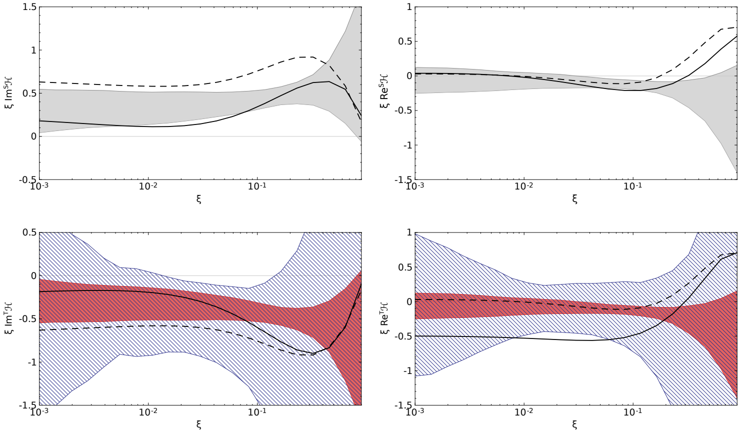

Figure: Imaginary (left) and real (right) part of DVCS (up) and TCS (down) CFF for $Q^2 = 2$ GeV^2 and $t = -0.3$ GeV^2 as a function of ξ. The shaded red (dashed blue) bands correspond to the data-driven predictions coming from the ANN global fit of DVCS data and they are evaluated using LO (NLO) spacelike-to-timelike relations. The dashed (solid) lines correspond to the GK GPD model evaluated with LO (NLO) coefficient functions.

TCS and Bethe-Heitler contribution to exclusive lepton pair photoproduction.

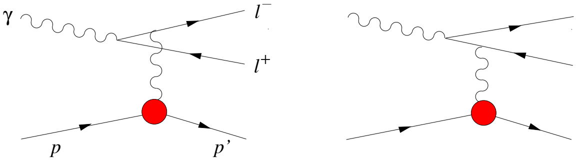

Figure: The Feynman diagrams for the Bethe-Heitler amplitude.

The cross-section for photoproduction of a lepton pair:

$$\frac{d\sigma}{dQ'^2\ dt\ d\phi\ d\cos\theta} = \frac{d\left(\sigma_{\mathrm{BH}} + \sigma_{\mathrm{TCS}} + \sigma_{\mathrm{INT}}\right)}{dQ'^2\ dt\ d\phi\ d\cos\theta}$$

TCS

Berger, Diehl, Pire, 2002

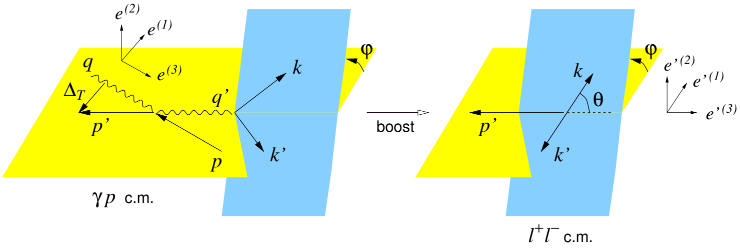

Figure: Kinematical variables and coordinate axes in the γp and $\ell^+\ell^-$ c.m. frames.

$$\frac{d\sigma}{dQ'^2\ dt\ d\phi\ d\cos\theta}$$

- Important to measure ϕ !
- BH dominates at θ close to 0 and π !

Interference

- B-H dominant for not very high energies (JLAB), at higher energies the TCS/BH ratio is bigger due to growth of the gluon and sea densities.

Pire, Szymanowski, JW PRD 83

Moutarde, Pire, Sabatié, Szymanowski, JW PRD 87

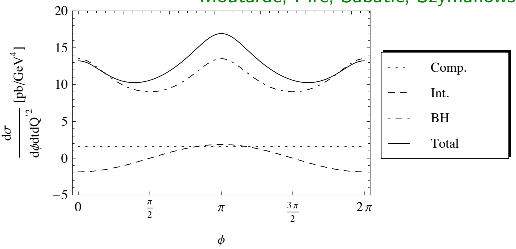

Figure: The differential cross section for $t = -0.2$ GeV^2 , $Q'^2 = 5$ GeV^2 , and integrated over $\theta \in (\pi/4, 3\pi/4)$ as a function of ϕ, for $s = 10^3$ GeV^2.

- The interference part of the cross-section for $\gamma p \to \ell^+ \ell^- p$ with unpolarized protons and photons is given by:

$$\frac{d\sigma_{INT}}{dQ'^2\, dt\, d\cos\theta\, d\varphi} \sim \cos\varphi \cdot \; \mathrm{Re}\,\mathcal{H}(\xi, t) \leftarrow \text{Sensitivity to the D-term!}$$

Charge asymmetry selects interference - in DVCS one needs positron beam, here this is given by the angular dependence!

Interference

R ratio:

$$R = \frac{2\int_0^{2\pi} \cos\phi \; d\phi \int_{\pi/4}^{3\pi/4} d\theta \, \frac{dS}{dQ'^2 dt d\phi d\theta}}{\int_0^{2\pi} \; d\phi \int_{\pi/4}^{3\pi/4} d\theta \, \frac{dS}{dQ'^2 dt d\phi d\theta}} \, ,$$

where S is the weighted cross section :

$$\frac{dS}{dQ'^2 dt d\phi d\theta} = \frac{L(\theta,\phi)}{L_0(\theta)} \frac{d\sigma}{dQ'^2 dt d\phi d\theta} \, ,$$

Forward Backward Asymmetry (from Pierre Chatagnon PhD thesis):

$$A_{FB}(\theta,\phi) = \frac{d\sigma(\theta,\phi) - d\sigma(180^\circ - \theta, 180^\circ + \phi)}{d\sigma(\theta,\phi) + d\sigma(180^\circ - \theta, 180^\circ + \phi)}$$

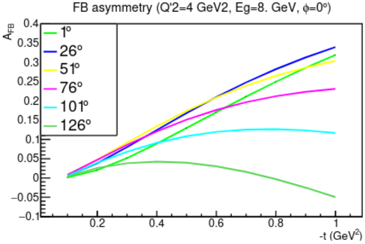

(a)

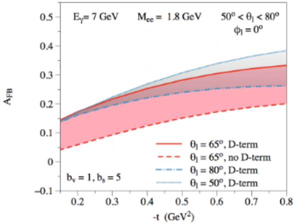

(b)

Unpolarized cross section

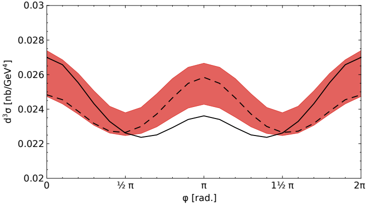

Figure: Differential TCS cross section integrated over $\theta \in (\pi/4, 3\pi/4)$ for $Q'^2 = 4$ GeV^2, $t = -0.1$ GeV^2 and the photon beam energy $E_\gamma = 10$ GeV as a function of the angle ϕ. In the left (right) panel the data-driven predictions evaluated using LO (NLO) spacelike-to-timelike relations are shown. The dashed (solid) lines correspond to the GK GPD model evaluated with LO (NLO) TCS coefficient functions (the curves are the same in both panels). Note the different scales for the upper and lower panels.

R ratio

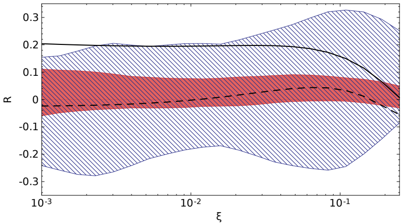

Figure: Ratio R evaluated with LO and NLO spacelike-to-timelike relations for $Q'^2 = 4$ GeV^2, $t = -0.35$ GeV^2 as a function of ξ.

Circular asymmetry

The photon beam circular polarization asymmetry:

$$A_{CU} = \frac{\sigma^+ - \sigma^-}{\sigma^+ + \sigma^-} \sim Im(H)$$

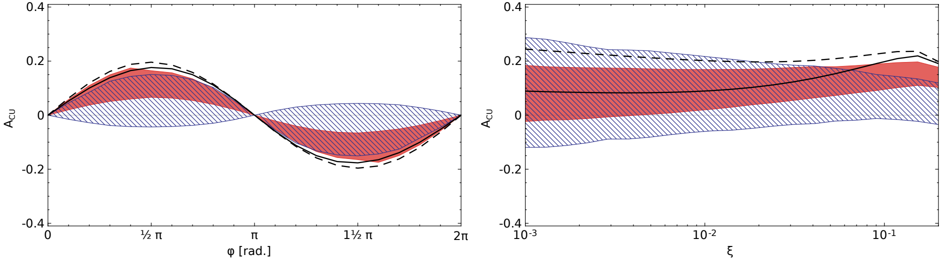

Figure: Circular asymmetry A_{CU} evaluated with LO and NLO spacelike-to-timelike relations for $Q'^2 = 4$ GeV^2, $t = -0.1$ GeV^2 and (left) $E_\gamma = 10$ GeV as a function of ϕ (right) and $\phi = \pi/2$ as a function of ξ. The cross sections used to evaluate the asymmetry are integrated over $\theta \in (\pi/4, 3\pi/4)$.

Transverse target asymmetry

$$\frac{d\sigma^{\mathrm{tpol}}_{\mathrm{INT}}}{dQ'^2 d(\cos\theta) d\phi dt d\varphi_S} \sim \sin\varphi_S \Im\Big[\mathcal{H} - \frac{\xi^2}{1-\xi^2}\mathcal{E} + \widetilde{\mathcal{H}} + \frac{t}{4M^2}\widetilde{\mathcal{E}}\Big].$$

The transverse spin asymmetry:

$$A_{UT}(\varphi_S) = \frac{\sigma(\varphi_S) - \sigma(\varphi_S - \pi)}{\sigma(\varphi_S) + \sigma(\varphi_S - \pi)},$$

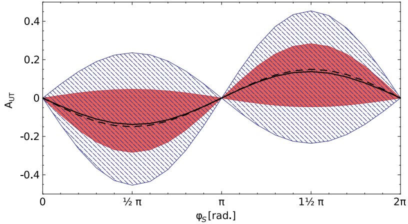

Figure: Transverse target spin asymmetry A_{UT} evaluated with LO and NLO spacelike-to-timelike relations for $Q'^2 = 4$ GeV^2, $t = t_0$ and $E_\gamma = 10$ GeV as a function of φ_S. The cross sections used to evaluate the asymmetry are integrated over $\theta \in (\pi/4, 3\pi/4)$.

Other experimental possibility - Ultraperipheral collisions

LHCb, CMS, ALICE, AFTER

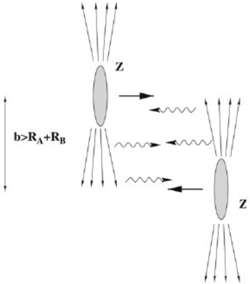

$$\sigma^{AB} = \int dk_A \frac{dn^A}{dk_A} \sigma^{\gamma B}(W_A(k_A)) + \int dk_B \frac{dn^B}{dk_B} \sigma^{\gamma A}(W_B(k_B))$$

TCS has the same final state as J/ψ, already measured in UPCs!

TCS at UPC

B.Pire, L.Szymanowski, J.Wagner, PRD86

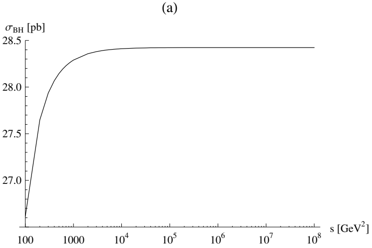

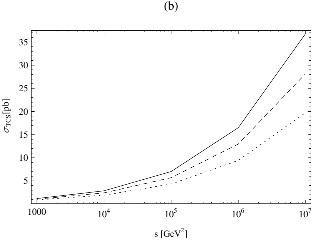

Figure: (a) The BH cross section (b) σ_{TCS} as a function of γp c.m. energy squared s

Cross section integrated over $\theta = [\pi/4, 3\pi/4]$, $\phi = [0, 2\pi]$, $t = [-0.05\,\mathrm{GeV}^2, -0.25\,\mathrm{GeV}^2]$, $Q'^2 = [4.5\,\mathrm{GeV}^2, 5.5\,\mathrm{GeV}^2]$, and photon energies $k = [20, 900]\,\mathrm{GeV}$ gives:

$$\sigma_{pp}^{BH} = 2.9\,\mathrm{pb} \qquad \sigma_{pp}^{TCS} = 1.9\,\mathrm{pb}\;.$$

Even better with pA collisions. Lansberg, Szymanowski, Wagner JHEP 09 (2015) 087

Summary

- TCS is a mandatory complementary measurement to DVCS, cleanest way to test universality of GPDs,
- Timelike-spacelike relations at LO/NLO gives us tools to use TCS data in DVCS CFF fits, with special sensitivity to Q^2 dependence,
- First data-driven and model-free predictions for TCS using global DVCS data
- Results from CLAS12 !!!
- EIC - TCS study in Yellow Report
- Possible also in UPCs in LHC.
- Other exclusive processes with dilepton:
  - TCS on neutron Boer, Guidal, Vanderhaeghen
  - backward TCS with TDA Pire, Semenov-Tian-Shansky, Szymanowski
  - Exclusive Drell-Yann Berger, Diehl, Pire
  - TCS on pion (with a Sullivan process)
  - Measurement of TCS should also make us more optimistic about the DDVCS Belitsky, Müller and Guichon, Guidal, Vanderhaeghen
- Natural extension : replace in final state high mass dilepton by high mass diphoton! Grocholski, Pedrak, Pire, Sznajder, Szymanowski, Wagner